

# Novel magnetic ordering in LiYbO<sub>2</sub> probed by muon spin relaxation

Eric M. Kenney<sup>1</sup>, Mitchell M. Bordelon<sup>2</sup>, Chennan Wang<sup>4</sup>, Hubertus Luetkens<sup>4</sup>, Stephen D. Wilson<sup>3</sup>, and Michael J. Graf<sup>1</sup>

<sup>1</sup> Department of Physics, Boston College, Chestnut Hill, Massachusetts, 02467, USA

<sup>2</sup> Materials Physics and Applications–Quantum, Los Alamos National Laboratory, Los Alamos, New Mexico, 87545, USA

<sup>3</sup> Materials Department, University of California, Santa Barbara, California, 93106, USA

<sup>4</sup> Laboratory for Muon Spin Spectroscopy, Paul Scherrer Institute, 5232 Villigen, Switzerland

## Abstract

The stretched diamond lattice material LiYbO<sub>2</sub> has recently been reported to exhibit two magnetic transitions ( $T_{N1} = 1.1$  K,  $T_{N2} = 0.45$  K) via specific heat, magnetization, and neutron scattering measurements [Bordelon et al., Phys. Rev. B **103**, 014420 (2021)]. Here we report complementary magnetic measurements down to  $T = 0.28$  K via the local probe technique of muon spin relaxation. While we observe a rapid increase in the zero-field muon depolarization rate at  $T_{N1}$ , we do not observe any spontaneous muon precession for  $T < T_{N1}$ , which is typically associated with long-range magnetic ordering. The depolarization rate in the ordered state shows a surprising sensitivity to magnetic fields applied along the initial spin polarization direction. Using a simple one-dimensional model, we show that these results are consistent with the unusual random-phase bipartite incommensurate magnetic structure proposed by Bordelon et al. for the intermediate temperature range  $T_{N2} < T < T_{N1}$ . We also find evidence for temperature-independent magnetic fluctuations persisting to our lowest temperatures, but no obvious signature of the transition or spontaneous muon precession at and below  $T_{N2}$ , respectively. This result is suggestive of quantum dynamics within a highly degenerate ground state.

While a variety of interesting phenomena are expected to occur in magnetically frustrated systems, there are relatively few material families that predictably host frustrated magnetism and typically systems order or freeze at finite temperatures [1–4]. There are even fewer frustrated 3D systems in the low-spin  $S = \frac{1}{2}$  limit. 3D frustration has mainly focused on magnetic pyrochlore lattices, such as the lanthanide materials  $Ln_2M_2O_7$ ,  $Ln$  = Lanthanide,  $M$  = Metal or Metalloid.[5] Magnetic frustration on diamond lattices has been relatively less researched.

Recently, Bordelon et al. [6] reported the successful synthesis of polycrystalline  $\text{LiYbO}_2$ , along with a detailed set of structural, specific heat, magnetization, and neutron scattering data. Structurally the system forms a stretched diamond lattice. The  $\text{Yb}^{3+}$  ions can be modeled as two interpenetrating face-centered cubic sublattices with a nearest-neighbor Heisenberg interaction  $J_1$  between sublattices and a next-nearest-neighbor interaction  $J_2$  within a sublattice. The  $\text{Yb}^{3+}$  ions have electronic moments with  $J_{\text{eff}} = \frac{1}{2}$  and  $\mu = 3.3 \mu_B$ . Above 1.1 K the system is paramagnetic, with a Curie-Wiess temperature of  $\Theta_{\text{CW}} = -3.4$  K. Specific heat showed a transition at 1.1 K, followed by a weaker second transition at 0.45 K, resulting in a modest frustration factor of  $f \approx 3$ . Neutron diffraction measurements show that below 450 mK the two  $\text{Yb}^{3+}$  sublattices order as a bipartite incommensurate spiral magnetic ordering with wave vector of  $K = (0.384, \pm 0.384, 0)$  for each sublattice, and a rotational phase-difference of  $0.58 \pi$  between the sublattices. This magnetic structure was shown to be well described within the framework of a Heisenberg  $J_1 - J_2$  Hamiltonian as applied to the stretched diamond lattice, with  $\frac{J_2}{|J_1|} \approx 1.42$ .

The intermediate state between 450 mK and 1.1 K is less well understood. Unusual neutron diffraction patterns in this temperature interval were best described by taking the low-temperature spiral state and randomizing the phase difference between the two  $\text{Yb}^{3+}$  sublattices.[6] This novel approach suggests that the  $\text{Yb}^{3+}$  moments first order within their respective sublattices at 1.1 K, and then the two independent sublattices lock into the aforementioned  $0.58 \pi$  phase difference below 450 mK, resulting in the two transitions in  $\text{LiYbO}_2$ . To our knowledge, this is the first time a two-step magnetic transition of this type has been proposed. The simple Heisenberg model cannot account for this phase, and its appearance was attributed to additional anisotropic exchange terms in the Hamiltonian. Finally, inelastic neutron scattering (INS) revealed the existence of low-energy fluctuations of about 1 meV down to 38 mK. These low-energy fluctuations persisted in applied fields up to 10 T, at which a field-polarized state was induced.

However, it was not clear from these results if the fluctuations were caused by conventional magnetic excitations within the ordered state or by more exotic mechanisms, e.g. fluctuations between degenerate ground states or within a ‘quantum spiral spin liquid’ state [7-9].

In this work we present positive muon spin relaxation ( $\mu^+$ SR) measurements as a local-probe complement to the bulk measurements reported in Ref. 6. Our results confirm that  $\text{LiYbO}_2$  magnetically orders at  $T_{N1} \sim 1.1$  K, but the spontaneous oscillatory depolarization in zero applied field that is typical for long-range magnetic order is absent. We present a simple model for muon depolarization spectra for incommensurate bipartite lattices and show that the random phase model proposed for the  $\text{LiYbO}_2$  magnetic structure would naturally suppress coherent muon spin oscillations, consistent with our observations. Moreover, we find that the muon depolarization is unusually sensitive to weak applied longitudinal fields despite the strong depolarization in zero field, which can also be qualitatively explained by the model mentioned above. Finally, we find persistent magnetic fluctuations down to  $T = 0.28$  K, but cannot resolve a second magnetic transition near 0.45 K. These measurements suggest that the system enters a highly degenerate ordered ground state.

A polycrystalline sample of  $\text{LiYbO}_2$  was prepared using a solid-state reaction between  $\text{Yb}_2\text{O}_3$  and  $\text{Li}_2\text{CO}_3$  as reported previously [6]. Sample purity was verified via x-ray diffraction and susceptibility measurements. The powder was pressed into a disk approximately 1 cm in diameter and 3 mm thick in an Ar-atmosphere glovebox, and minimal exposure to air was maintained at all times.

The  $\mu^+$ SR experiments were performed at the Paul Scherrer Institute using the General Purpose Surface-Muon (GPS) [10] and Dolly instruments on the  $\pi\text{M3}$  and  $\pi\text{E1}$  beamlines, respectively, with measurements to 1.5 K in a gas flow cryostat (GPS) and 280 mK in an Oxford Heliox  $^3\text{He}$  cryostat (Dolly). The samples were mounted on 25- $\mu\text{m}$  thick copper foil in order to enhance thermalization at low temperatures. Measurements were performed in longitudinal spin-polarization mode with the initial muon polarization anti-parallel to the beam momentum. Data were analyzed using the MUSRFIT program [11].

The time-dependent muon depolarization between 40 K and 0.28 K are shown in Fig 1. Above 10 K the depolarization is temperature independent, and dominated by the Li nuclei. It is well described by

$$A(t) = A_0[(1 - F_B) G_{KT}(t)e^{-\lambda t} + F_B e^{-\lambda_B t}] . \quad (1)$$

The function  $G_{KT}(t)$  is the Gaussian Kubo-Toyabe[12–14] given by

$$G_{KT}(t) = \frac{1}{3} + \frac{2}{3}(1 - \sigma_N^2 t^2)e^{-\frac{\sigma_N^2 t^2}{2}} . \quad (2)$$

The first term in Eq. (1) describes muons depolarizing in the sample, while the second term accounts for a fraction  $F_B$  of muons landing in the cryostat and sample holder. For data taken in GPS,  $F_B$  is negligibly small, while  $F_B = 0.15(3)$  and  $\lambda_B = 0.27 \mu\text{s}^{-1}$  are obtained in Dolly. We find  $\sigma_N = 0.163(1) \mu\text{s}^{-1}$ , typical for compounds containing lithium, which has a fairly large nuclear moment of  $3.3 \mu_N$ . An additional exponential depolarization is present in the sample, with  $\lambda = 0.17(3) \mu\text{s}^{-1}$  in this temperature range, presumably due to fluctuating  $\text{Yb}^{3+}$  moments. In the crossover region between 10 and 2 K, the  $\text{Yb}^{3+}$  moments begin to slow and thus dominate the local field and muon depolarization. We note this temperature range corresponds to the broad maximum in specific heat originating from the onset of electronic correlations [6].

We now focus on our primary region of interest  $T < 2$  K. In Fig. 2 we show representative short-time depolarization curves. Here we see an abrupt change at 1.1 K, signaling the onset of magnetic order. The data is noteworthy for the lack of spontaneous muon precession as typically observed in materials with long-range magnetic order. In the inset we show a high-resolution curve taken at short times at  $T = 0.28$  K, and the lack of any oscillations is clear. The data below 2 K are well described by the phenomenological function

$$A(t) = A_0 \left\{ [1 - F_B] \left( (1 - f_\lambda) e^{-\frac{(\sigma t)^2}{2}} + f_\lambda e^{-\lambda t} \right) + F_B e^{-\lambda_B t} \right\}, \quad (3)$$

as shown by the solid lines in Figs. 1 and 2. In Fig. 3 we show the parameters  $\sigma$ ,  $\lambda$ , and  $f_\lambda$  as a function of temperature. The abrupt change in all three parameters at 1.10 K is clear. A fraction  $(1 - f_\lambda)$  of muons are rapidly depolarizing with an initially positive curvature approximated by a Gaussian decay, characteristic of a quasi-static array of densely packed moments. At the lowest temperatures  $\sigma$  is roughly 45 MHz, indicating a characteristic internal field of order  $\sigma/\gamma_\mu = 530$  G;  $\gamma_\mu = 0.08514 \text{ MHz/G}$  is the muon gyromagnetic ratio. A fraction  $f_\lambda = \frac{1}{3}$  (termed the ‘tail’) is expected and observed, below 1 K, representing the ensemble-averaged fraction of muons lying parallel to the local magnetic field, with decay caused by magnetic fluctuations and/or dilute

magnetic impurities in the sample. Within the muon time window, none of the parameters clearly indicate any transition at  $T = 0.45$  K where a weak anomaly is observed in specific heat [6].

In Fig. 4, we show results for the depolarization at  $T = 0.28$  K for several magnetic fields applied along the initial muon spin polarization direction (longitudinal field, or ‘LF’). Depolarization is suppressed when the LF is comparable to or greater than the internal field experienced by the muon, resulting in an increase in  $f_\lambda$ . A small field of 50 G immediately suppresses some of the long-time depolarization, due in part to the weakly magnetic background contribution. However, the detailed LF response is not well-described by the ‘standard’ model [2], and we will elaborate on this in the discussion below. We also note that a slow relaxation of the tail remains even at higher fields, due to depolarization in the sample by magnetic fluctuations. Such fluctuations were observed via neutron scattering in Ref. 6. At LF values of several hundred Gauss, the tail then lifts further, as expected for an internal field of order 530 G and inferred from our fit results at low temperatures.

We now discuss our  $\mu^+$ SR results in the context of the observations reported in Ref. 6. Our results are clearly consistent with the onset of a phase transition at 1.1 K, and the sharpness of this transition (see Fig. 3) suggests that there is very little chemical or magnetic disorder. Nonetheless, no spontaneous coherent muon precession is observed. Qualitatively, one might expect the complex nature of the magnetic order reported in Ref. 6 to suppress these oscillations. Motivated by the highly unusual proposed structure for  $T_{N2} < T < T_{N1}$  based on the neutron scattering results, we present a simple model to describe muon depolarization in this random-phase bipartite incommensurate (RPBI) state. We approximate the internal field distribution as two identical, but independent, incommensurate internal field distributions. The internal field distribution seen by the muon ensemble,  $D_{\text{RPBI}}(B_{\text{loc}})$ , is then described by the convolution of these two internal field distributions:

$$D_{\text{RPBI}}(B_{\text{loc}}) = (D_{\text{inc.}} * D_{\text{inc.}})(B_{\text{loc}}) \quad (4)$$

where  $D_{\text{inc.}}(B_{\text{loc}})$  is the basic model for the field distribution seen by muons inside an incommensurate magnet [15]:

$$D_{\text{inc.}}(B_{\text{loc}}; B_{\text{max}}) = \begin{cases} \frac{1}{\pi} \frac{1}{\sqrt{B_{\text{max}}^2 - B_{\text{loc}}^2}}, & -B_{\text{max}} < B_{\text{loc}} < B_{\text{max}} \\ 0, & \text{Otherwise} \end{cases} \quad (5)$$

Equation (4) can be solved analytically. The result is a *Complete Elliptical Integral of the First Kind*,  $K[x]$ , and we find

$$D_{\text{RPBI}}(B_{\text{loc}}; B_{\text{max}}) = \frac{4}{\pi^2} K \left[ 1 - \left( \frac{B_{\text{loc}}}{2B_{\text{max}}} \right)^2 \right] \{-2B_{\text{max}} \leq B_{\text{loc}} \leq 2B_{\text{max}}\} \quad (6)$$

We plot the field distributions for  $D_{\text{inc.}}$  and  $D_{\text{RPBI}}$  in Figure 5.

It can easily be shown (see Supplemental Material) that the depolarization function for this distribution is

$$P(t) = \frac{1}{3} + \frac{2}{3} J_0^2(\gamma_\mu B_{\text{max}} t) \quad (7)$$

where  $B_{\text{max}}$  is the asymptotically maximum field produced by a single magnetic sublattice and  $\gamma_\mu$  is the muon gyromagnetic ratio.

In the case of slow spin dynamics, such as the fluctuations observed in INS at low temperatures, static polarization functions generalize by multiplying the static tail by an exponential:

$$P(t) = \frac{1}{3} e^{-\lambda t} + \frac{2}{3} J_0^2(\gamma_\mu B_{\text{max}} t). \quad (8)$$

For experimental data with a background, the asymmetry function then becomes

$$A(t) = A_0 \left[ \{1 - F_B\} \left( (1 - f_\lambda) J_0^2 + f_\lambda e^{-\lambda t} \right) + F_B e^{-\lambda_B t} \right]. \quad (9)$$

where  $f_\lambda \cong \frac{1}{3}$ . This corresponds to our phenomenological function in Eq. (3), but with the Gaussian factor replaced by  $J_0^2$ .

In figure 5 we compare the resulting depolarization functions to the data at 550 mK along with phenomenological Gaussian fits described above by placing the fit parameters from equation (3) into (9). The resulting oscillations in the Bessel-squared model are smaller than the line-width of our data, even without considering other potential sources of magnetic disorder which would further suppress oscillations, such as magnetic defects. Finally, we note that both the Gaussian and Bessel-squared functions have the same short-time limit

$$e^{-\frac{(\sigma t)^2}{2}} \approx J_0^2(\sigma t) \approx 1 - \frac{1}{2} \sigma^2 t^2 \quad (8)$$

which would explain the good agreement of our phenomenological fit function Eq. 3 to the data.

The unusual shape of  $D_{\text{RPBI}}(B_{\text{loc}}; B_{\text{max}})$  will also affect the depolarization in applied longitudinal fields. The application of a LF  $B_{\text{LF}}$  comparable to the internal field  $B_{\text{int}}$  will increase the fraction  $f_\lambda$ , and when  $B_{\text{LF}} \gg B_{\text{int}}$  one finds  $f_\lambda \sim 1$ . This has been calculated for standard magnetic materials with long-range order [16] or disorder [15]. We expect that for the RPBI model the

system will be much more sensitive to the application of a LF due to the peak in the field distribution at zero. In Fig. 6a we show the fraction  $f_\lambda$  as a function of applied longitudinal fields at  $T = 0.28$  K, along with the known responses for a conventional magnet and our calculated responses for a simple incommensurately ordered magnet and one with RPBI order. Indeed, we find that the qualitative response is best described by the RPBI model. However, the gross disagreement at high fields with all models illustrates that the effects of dynamics in this system are strong and cannot be ignored.

The dynamical effects on  $P_{LF}$  may be accounted for by using previously established theory on other related materials. For example,  $\text{Yb}_2\text{Ti}_2\text{O}_7$  is another geometrically frustrated system with persistent spin fluctuations deep in the ordered phase and an unusual magnetic order[17].  $\text{Yb}_2\text{Ti}_2\text{O}_7$  exhibits an unusual form of secondary dynamics known as ‘sporadic dynamics,’ which results in linear screening [18] of applied longitudinal fields. For  $\text{Yb}_2\text{Ti}_2\text{O}_7$ , the screening factor is  $B_{LF}/B_{\text{ext}} \cong 0.17$  [19]. This suggests that we try a linear scaling factor,  $B_{LF} = \alpha B_{\text{ext}}$ , as our zero- and longitudinal-field data is clearly neither in the strong dynamical limit, nor well described by a reasonably sized internal field. Figure 6b shows good quantitative agreement with a scaling factor  $\alpha = 1/3$ .

Finally, we discuss lack of spontaneous muon precession below  $T_{N2} = 0.45$  K, or indeed any pronounced signature of that transition, in the  $\mu^+\text{SR}$  data. Although the system is proposed to be phase-locked below 0.45 K rather than random-phase, we note that the propagation direction of the doubly degenerate wave vector  $(0.384, \pm 0.384, 0)$  determined from neutron diffraction could be in any direction within the  $ab$ -plane. This allows for a highly degenerate ground state of spiral domains with the same wave vector. The degeneracy would manifest as a *de facto* phase-randomization in the  $\mu^+\text{SR}$  data (see the *Supplemental Information* for additional discussion), explaining the close similarity between our RPBI model and the data in the  $T < 0.45$  K temperature regime. Such a highly degenerate spiral ground state, combined with the observation of a weak thermodynamic signature at  $T_{N2}$  and dynamical behavior from  $\mu^+\text{SR}$  and INS, present an intriguing possibility of ‘quantum spiral spin liquid’ ground state, as recently proposed for  $\text{NiRh}_2\text{O}_4$  [9].

Summarizing, we performed local probe  $\mu^+\text{SR}$  measurements on  $\text{LiYbO}_2$  to complement recent neutron, bulk magnetic, and thermodynamic measurements [6]. We find clear signatures of the sharp magnetic transition at 1.1 K, but none for the second observed transition at 0.45 K. No spontaneous muon precession is observed for  $T < 1.1$  K, and we propose a simple model based on the novel magnetic structure reported in Ref. [6] that is consistent with this result. This model is

also consistent with our observation of unusual sensitivity of the muon depolarization to applied longitudinal magnetic fields. Finally, our results confirm the presence of magnetic fluctuations down to  $T = 0.28$  K, suggesting that despite the relatively low frustration factor of  $f \sim 3$ ,  $\text{LiYbO}_2$  fluctuations amongst allowed spiral states/configurations may remain significant. Future studies on single crystals to lower temperatures will help to clarify many of the unanswered questions regarding this material.

### **Acknowledgements**

This work is based on experiments performed at the Swiss Muon Source S $\mu$ S, Paul Scherrer Institute, Villigen, Switzerland. MMB and SDW were supported by the US Department of Energy Office of Basic Energy Sciences, Division of Materials Science and Engineering under award DE-SC0017752.



## References

- [1] Z. Ma, K. Ran, J. Wang, S. Bao, Z. Cai, S. Li, and J. Wen, *Chin. Phys. B* **27**, 106101 (2018).
- [2] H. Takagi, T. Takayama, G. Jackeli, G. Khaliullin, and S. E. Nagler, *Nat. Rev. Phys.* **1**, 4 (2019).
- [3] J. Wen, S.-L. Yu, S. Li, W. Yu, and J.-X. Li, *Npj Quantum Mater.* **4**, 1 (2019).
- [4] L. Savary and L. Balents, *Rep. Prog. Phys.* **80**, 016502 (2017).
- [5] T. Biesner and E. Uykur, *Crystals* **10**, 1 (2020).
- [6] M. M. Bordelon, C. Liu, L. Posthuma, E. Kenney, M. J. Graf, N. P. Butch, A. Banerjee, S. Calder, L. Balents, and S. D. Wilson, *Phys. Rev. B* **103**, 014420 (2021).
- [7] L. Balents, *Nature* **464**, 199 (2010).
- [8] X.-P. Yao, J. Q. Liu, C.-J. Huang, X. Wang, and G. Chen, *Front. Phys.* **16**, 53303 (2021).
- [9] F. Buessen, M. Hering, J. Reuther, and S. Trebst, *Phys. Rev. Lett.* **120**, 057201 (2018).
- [10] A. Amato, H. Luetkens, K. Sedlak, A. Stoykov, R. Scheuermann, M. Elender, A. Raselli, and D. Graf, *Review of Scientific Instruments* **88**, 093301 (2017)]
- [11] A. Suter and B. M. Wojek, *Phys. Procedia* **30**, 69 (2012).
- [12] *Muon Science: Muons in Physics, Chemistry and Materials*, S.L. Lee, S.H. Kilcoyne, R. Cywinski, (Scottish Universities Summer School in Physics & Institute of Physics Pub., Philidelphia, PA, 1999)
- [13] Y. J. Uemura, *MSR Relaxation Functions in Magnetic Materials*, S.L. Lee, S.H. Kilcoyne, R. Cywinski, (Scottish Universities Summer School in Physics & Institute of Physics Pub., Philidelphia, PA, 1999)
- [14] P. D. de Réotier and A. Yaouanc, *J. Phys. Condens. Matter* **9**, 9113 (1997).
- [15] A. Yaouanc and P. Dalmas De Réotier, *Muon Spin Rotation, Relaxation, and Resonance: Applications to Condensed Matter* (Oxford University Press, New York, NY, 2011).
- [16] F. L. Pratt, *J. Phys. Condens. Matter* **19**, 456207 (2007).
- [17] P. Dalmas de Réotier, A. Maisuradze, and A. Yaouanc, *J. Phys. Soc. Jpn.* **85**, 091010 (2016).
- [18] Y. J. Uemura, A. Keren, K. Kojima, L. P. Le, G. M. Luke, W. D. Wu, Y. Ajiro, T. Asano, Y. Kuriyama, M. Mekata, H. Kikuchi, and K. Kakurai, *Phys. Rev. Lett.* **73**, 3306 (1994).
- [19] P. Dalmas de Réotier, V. Glazkov, C. Marin, A. Yaouanc, P. C. M. Gubbens, S. Sakarya, P. Bonville, A. Amato, C. Baines, and P. J. C. King, *Phys. B Condens. Matter* **374–375**, 145 (2006).

## Figures

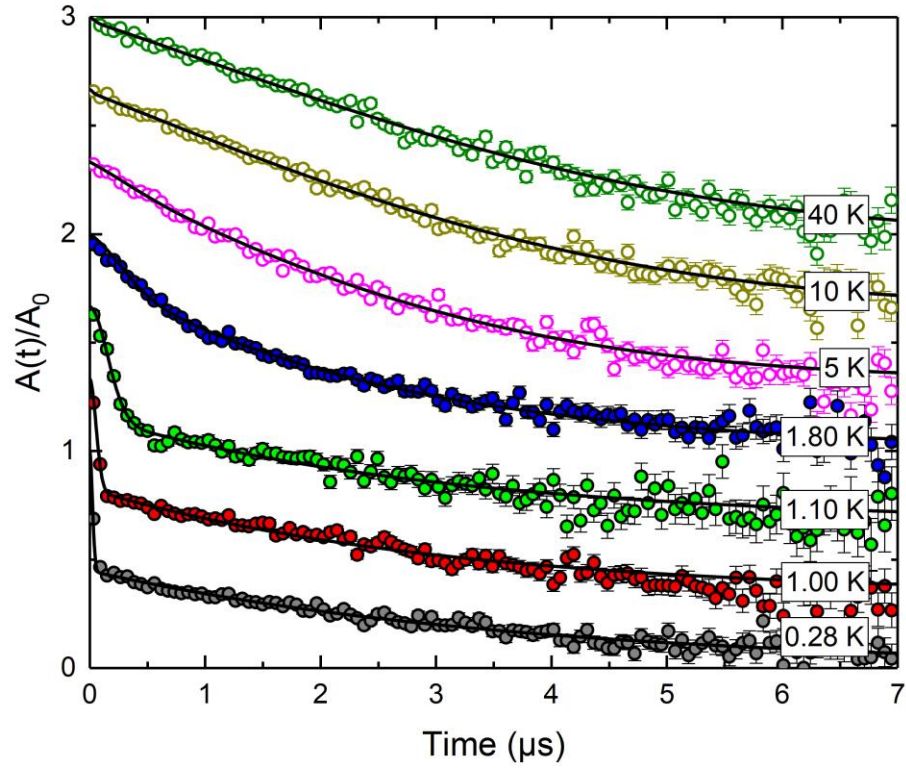


Figure 1: Zero field depolarization spectra of LiYbO<sub>2</sub> measured on the Dolly (solid circles) and GPS (empty circles) spectrometers with fits as described in text (solid lines). Curves are offset by  $1/3$  for clarity.

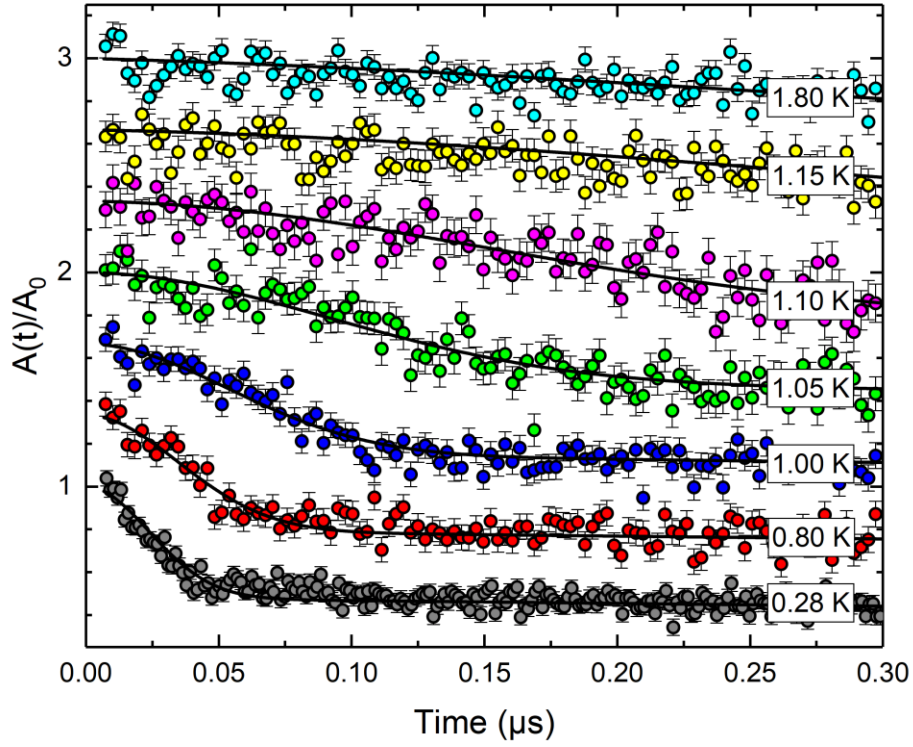


Figure 2: Short-time zero-field (ZF) asymmetry spectra plotted from 0  $\mu\text{s}$  to 0.3  $\mu\text{s}$ . Spectra were measured on Dolly and range from 0.28 K to 1.8 K. We observe a sharp transition between 1.10K and 1.15K. At 0.28 K the time-gating was adjusted to increase temporal resolution. No oscillations or dips are seen in the spectra, despite improved resolution. Curves are offset by 1/3 for clarity.

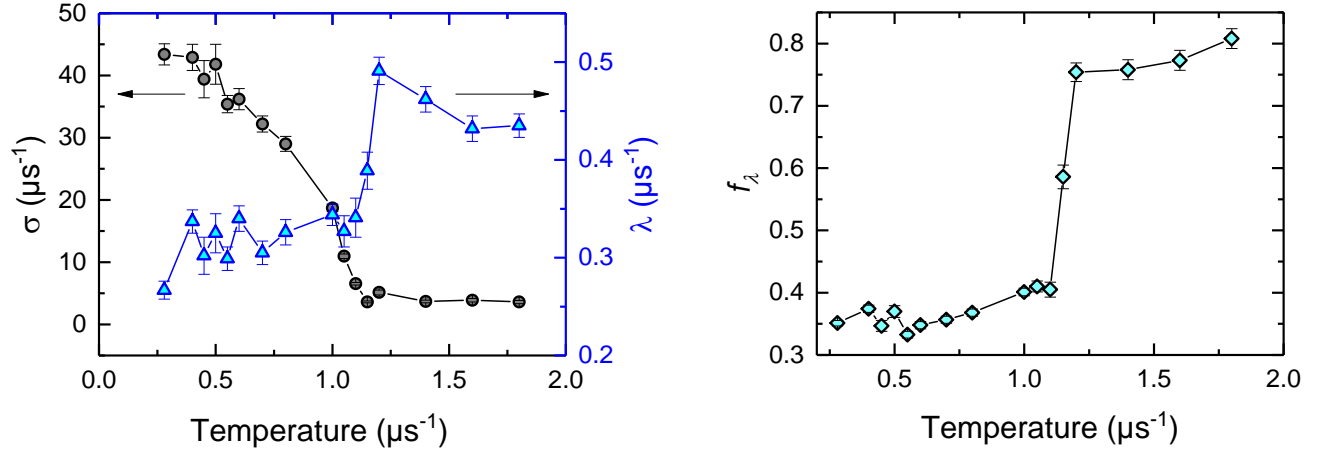


Figure 3: Temperature dependence of the fit parameters described in the main text. The exponential rate  $\lambda$  and its fraction  $f_\lambda$  describes the long-time decay of the asymmetry, presumably due to quasi-static fluctuations, while the Gaussian rate  $\sigma$  describes the short-time behavior due to static order. The drop of  $f_\lambda$  to 1/3 at the transition is consistent with a long-range ordering transition reducing dynamics, resulting in the appearance of a weakly damped 1/3-tail.

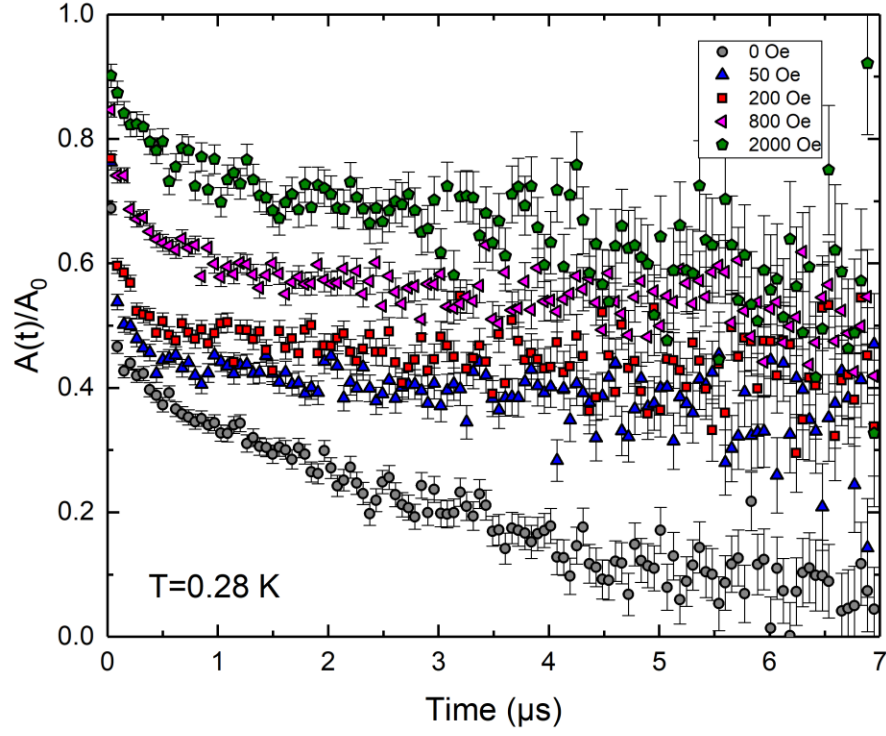


Figure 4: Longitudinal Field  $\mu^+$ SR Spectra at 0.28K. The initial lifting of the asymmetry spectra corresponds to the suppression of static disorder or quasi-static fluctuations. The small lifting of the asymmetry between 50 Oe to 800 Oe allows us to estimate the internal field strength associated with the rapid decay to be roughly 500 Oe.

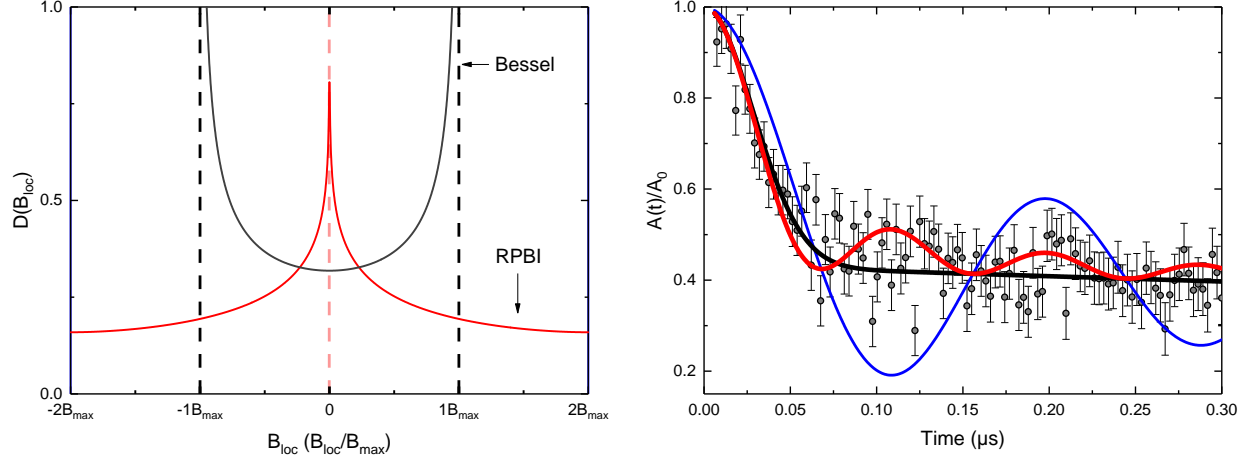


Figure 5: (Left) Field distributions  $D(B_{\text{loc}})$  for a simple incommensurate magnet (Bessel) and the RPBI distribution, as described in the text. (Right) Asymmetry plots at  $T = 550$  mK plotted against the Bessel and Bessel squared polarization functions described in the text. The parameters used are obtained from the shown Gaussian fit. For the Bessel polarization, we take  $\gamma_{\mu} B_{\text{max}} = \sqrt{2} \sigma$  in accordance with the short-time expansions of  $J_0$  and  $e^{\frac{-\sigma^2 t^2}{2}}$ .

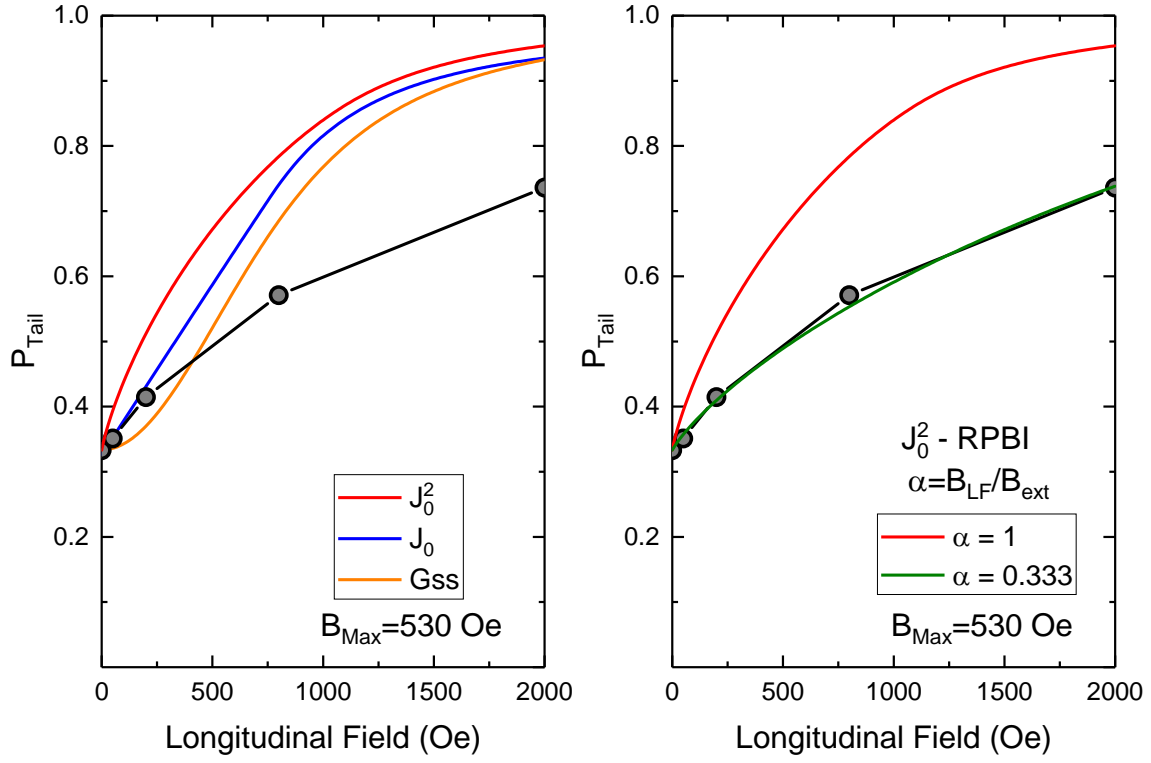


Figure 6: (Left) Longitudinal field dependence of the static tails for the data shown in Figure 4 (grey points with grey lines to guide the eye.) Overlaid is the calculated LF dependence for the field distributions in the text, given the fit parameters extracted from the fit at 0.28 K. The used internal field values are derived from the fitted depolarization rate. The lack of high-field agreement in any model indicates the presence of dynamics, despite the gaussian-like line-shape in zero-field. (Right) The LF tail recalculated using a linearly screened field with  $\alpha = \sim 1/3$ .